

A Gated Microchannel Plate Soft X-Ray Imaging System for a Laser Plasma Experiment

Bing SHAN*, Zenghu CHANG, Jinyuan LIU, Xiuqin LIU, Shengshen GAO, Youlai REN and Wenhua ZHU

State Key Laboratory of Transient Optics Technology, Xi'an Institute of Optics and Precision Mechanics,
Chinese Academy of Sciences, Xi'an, China

(Received December 25, 1997; accepted for publication March 18, 1998)

A picosecond soft X-ray imaging system for a laser plasma experiment which is convenient for practical use is developed. The system, based on a gated microchannel plate (MCP) with four 6-mm-wide stripline cathodes is capable of capturing multiframe soft X-ray images at time resolution of 60–100 ps and spatial resolution of 15 lp/mm. During design and construction of the system, emphasis was placed on reliability and operating convenience. The four gating pulses for each stripline were generated by a single avalanche transistor circuit, ensuring a steady time sequence and the same waveform for each pulse. The transmission characteristics of the four striplines were adjusted to be identical by monitoring the time domain reflectometry (TDR) of each stripline. The construction of the pulser and striplines in this manner allowed for both timing and sensitivity consistency of the gating for the four striplines. A pinhole system was equipped in front of the imager with precise control and flexible pinhole illumination, making the alignment and adjustment of the pinhole array very easy. The system was used in a high-power laser plasma experiment and results were obtained both with the pinhole and pinhole grating array.

KEYWORDS: plasma diagnostics, gated MCP, picosecond

1. Introduction

Picosecond gated microchannel plate (MCP) framing cameras have been rapidly developed during the past decade and have become one of the most important pieces of equipment for soft X-ray diagnostics of high temperature-plasma.^{1–8)} These cameras based on a gated MCP coated with stripline cathode can resolve broadband X-rays (1–5 keV) with very high time and spatial resolution, and have been routinely used in laser plasma experiments in many laboratories.

As illustrated in Fig. 1(a), the gated MCP camera is composed of a proximity focused MCP imager with parallel stripline type cathodes and a pulser providing gating pulses for each stripline. During laser plasma experiments, the pinhole or pinhole grating array produces many X-ray images on the stripline. These X-ray images are converted into electron images by the X-ray cathode coated on the stripline. At the same time, high voltage gating pulses are generated synchronously with the X-ray signal by a pulser and propagated along the striplines with different time delay to gate these electron images passing the MCP at different times. The gated electron images are then converted into optical images by a phosphor screen and recorded on film or charge coupled device (CCD) camera.

It can be seen that the intervals between the different images are determined by the time difference between the gating pulses on each image and can be adjusted by the delay of each pulse. The exposure time of each image was mainly determined by the pulse width. The size of each image on MCP is limited by the stripline width, which is mainly constrained by the driving ability of the gating pulses. The transmission impedance of the stripline will decrease with increasing stripline width, and a higher voltage pulse is requested to maintain a usable gain of the gating.

The key techniques used for the camera are high-voltage picosecond pulses for MCP gating and the transmission structure in the imager. The early works of MCP gating usually used a meander stripline cathode on MCP and gated it with

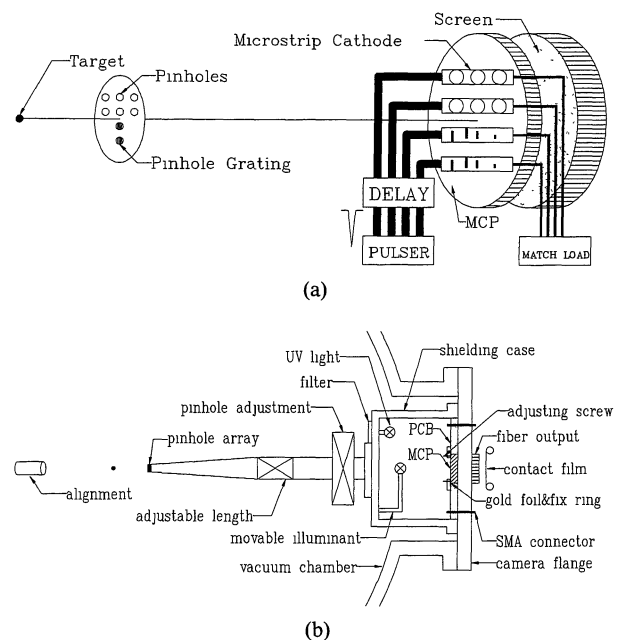


Fig. 1. Working principle and structure of the gated MCP framing system. (a) Working principle of the gated MCP framing camera. (b) Structure of the gated MCP system.

a single pulse. This is easier to fabricate as only one gating pulse is requested. However, it can only perform a measurement during a finite interval of about 1 ns because of the limited length of the stripline. In addition, there exists the problem of gain decrease along the stripline because of the transmission loss of the gating pulse.^{1,2,5,6)} The configuration of a multi-stripline type enable a longer period of measurement and improved gain uniformity.⁴⁾ However timing and sensitivity inconsistencies may exist between the striplines because they are driven by four separate gating pulses. Timing inconsistency is caused by jitters between pulses and sensitivity inconsistency can be induced by the difference between the transmission characteristics or response sensitivity of striplines and pulse waveforms.

During the experiment, because of the limited size of the stripline cathode, precise alignment of the pinholes with the

*Present address: Department of Electronic Engineering, Gunma University, Kiryu, Gunma 376, Japan. E-mail: shan@el.gunma-u.ac.jp

target and striplines is requested to obtain soft X-ray images on the MCP active area. However, the alignment is always difficult because there are many pinholes to be aligned and the stripline cathode is rather narrow, and the tiny pinholes are very hard to observe during the alignment. This makes the camera inconvenient in practical use.

In the present paper, a multiframing camera system with high performance reliability and operating convenience has been described. The system was equipped with a pinhole adjustment system with both manual and stepping motor controls, which enables easy and quick alignment of pinhole array with the target and striplines. The consistent response of the four striplines was emphasized in design and construction. The camera system was examined in a laser plasma experiment for soft X-ray imaging with 12 successive frames.

2. Construction of the System

Figure 1(b) shows the structure of the camera system. For a compact design, the system is composed of an imaging part and a control unit. The proximity focused imager welded on a vacuum flange is the core of the imaging part and is covered by a shielding case. The imager has four stripline cathodes coated on the MCP and fine transmission paths which correspond to each stripline. The pinhole adjustment device is fixed on the shielding case in front of the imaging part. The moveable illuminant for the pinhole array alignment and the UV light for static examination of the imager are installed on the inner side of the shielding case. The control unit provides power and controls for the camera, including power to the phosphor screen, gating pulses to the MCP, bias and static checking power for the MCP, control signals for stepping motors, power for illumination, and UV light.

The configuration of the four stripline cathodes implies that four separate high-voltage pulses are requested to gate each stripline. As mentioned above, the key technical factor in the design and construction is the consistency of the four striplines. This demands that careful attention should be paid to obtaining identical responses of the four cathodes, identical waveforms of the four gating pulses, identical transmission characteristics of the four striplines, and minimizing jitters between the gating pulses.

2.1 MCP imager

In the imager, the MCP is 56 mm in diameter and 0.5 mm in thickness with the microchannel diameter of $12\ \mu\text{m}$. The width of the four coated stripline cathodes is 6 mm, and the effective length of the stripline is 36 mm. This means that the largest size of an image on the MCP is $36\ \text{mm} \times 6\ \text{mm}$. The P20 phosphor screen was fabricated on a fiber-optic output window.

The stripline cathode was formed by coating Cu and Au with a mold masked on the MCP. We first coated the MCP with Cu until the electric impedance of each stripline was under $0.5\ \Omega$, then coated the Cu striplines with $800\ \text{\AA}$ Au as an X-ray photocathode.

For the 6-mm-wide stripline on the MCP, the resultant transmission impedance is about $17\ \Omega$. To match the $50\ \Omega$ connectors and the pulse generator, a stripline transformer is utilized to change the transmission impedance from $50\ \Omega$ to $17\ \Omega$ on the input side of the four striplines and change the impedance from $17\ \Omega$ to $50\ \Omega$ on the output side. This

was done by changing the width of the stripline exponentially from 1.32 mm on the $50\ \Omega$ connector side to 6 mm on the MCP side. The transformer is manufactured on a special printed circuit board (PCB) with a dielectric constant of 2.65, which is almost the same as the dielectric constant of the MCP used by us. Therefore, the stripline on the PCB and the MCP matched not only in impedance but also in width. This was very convenient for connecting the stripline on the PCB and the MCP. We used a $20\text{-}\mu\text{m}$ -thick gold foil to connect the striplines from the PCB to the MCP. A ceramic fixing ring was fixed on the MCP/PCB joint, securing the MCP and the gold foil in the imager. Eight adjusting screws in the fixing ring just at the eight ends of the four striplines on the MCP. The transmission characteristics can be adjusted by the screws pressing on each gold foil at the stripline end. Eight vacuum sealed SMA microstripline connectors were fixed on the flange and at the end of the stripline transformer on the PCB acting as the connectors to the pulser and matched load.

Figure 2 shows (a) the stripline structure in the imager and (b) the measured time domain reflectometry (TDR) curves of the four transmission paths. As shown in Fig. 2, the striplines are symmetrical around the input and output side of the path.

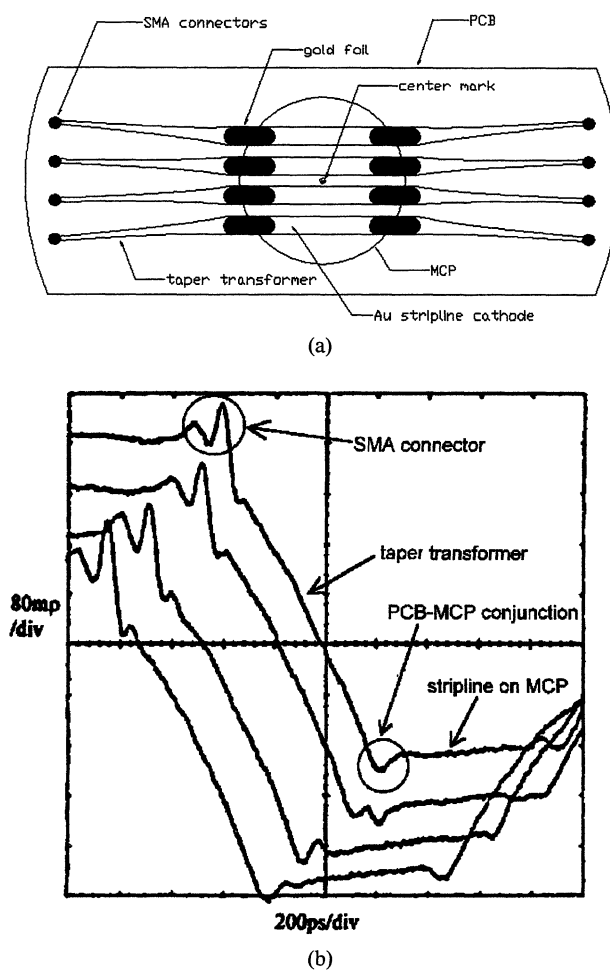


Fig. 2. Transmission structure in the imager. (a) Stripline structure in the imager. The striplines on the MCP and PCB were connected by gold foils. The eight ends of the striplines were directly soldered to the vacuum sealed SMA microstripline connectors. The width of striplines ranges from 1.32 mm ($50\ \Omega$) at the connectors to 6 mm ($17\ \Omega$) at MCP, and to 1.32 mm at the output connector. (b) Measured Time Domain Reflectometry (TDR) of the four paths. Reflections at each part were marked.

To maintain the consistency between the four striplines, we carefully adjusted the transmission properties of the striplines under the TDR monitor. It can be seen in the TDR result that there is little difference between the four paths and the reflection at the joint is small.

The distance from the output surface of the MCP to phosphor was 0.5 mm. The output surface of the MCP was coated with a dielectric layer to raise the working voltage of the MCP/screen gap.⁹⁾ A discrimination plate was used to measure the spatial resolution. The quartz glass plate contained with bars with different spacing ranging from 1 lp/mm to 30 lp/mm. We masked the plate on the MCP and obtained a modulated illumination on the MCP with UV light. The output pattern on the screen was then analysed to obtain the spatial resolution. The measured static spatial resolution of the camera was 15 lp/mm of 10% modulation. We also tested the equality of the response of the four stripline cathodes by evenly-distributed UV light. The equality was measured with DC bias to be better than 5%.

2.2 Pulse generator

The key specification of the framing camera is the exposure time, which is mainly determined by the gating pulse. The four gating pulses were generated by a sharpening diode circuit driven by a single step pulser. The step pulser is of a marx bank type composed of avalanche transistor 2N5551.

As mentioned above, the four gating pulses should be identical to ensure the consistency of the corresponding gating of the four striplines. This allows for the identical waveforms and fixed time sequences of the four pulses. We tried to use four separate circuits to generate the pulses, but it was impossible to maintain steady time sequences of the pulses because of circuit jitters, and it was difficult to adjust the four pulses to the same waveform. Due to instability and jitters which are mainly caused by the first stage avalanche transistor circuit, we tried to use one avalanche transistor circuit to drive several sharpening diode circuits to obtain the four gating pulses.

The circuit structure and measured pulses are shown in Figs. 3(a) and 3(b). A marx-bank type avalanche transistor circuit was used to obtain a parallel output of two identical step pulses of about 3 kV amplitude. The two step pulses were then modified by a second-stage circuit to improve the rising edge and elevate the amplitude. Next, the modified pulses were used to drive two pulse forming circuits. As shown in the figures, one forming circuit generates two gating pulses from two symmetrically arranged capacitors. Therefore, it is very easy to adjust the capacitors to obtain two identical pulses from one forming circuit. The four gating pulses were obtained by choosing two suitable diode circuits.

The diode circuit has a simple form as drawn in the figure, but is very critical to the structure. We used the 1N5408 diode which undergoes a very fast trapped plasma avalanche transit-time (TRAPATT) avalanche breakdown when applied with a fast step pulse.^{10,11)} In the third-stage pulse forming circuit, the plastic package and lead of the diode were removed to minimize distribution parameters. The amplitude and width of the output pulse can be adjusted by changing the capacitor and inductor value in the circuit.

Two (out 1 and out 3) of the four pulses are shown in Fig. 3(b), the other two pulses originated from the same diode circuit as the two displayed in the figure. The measurement

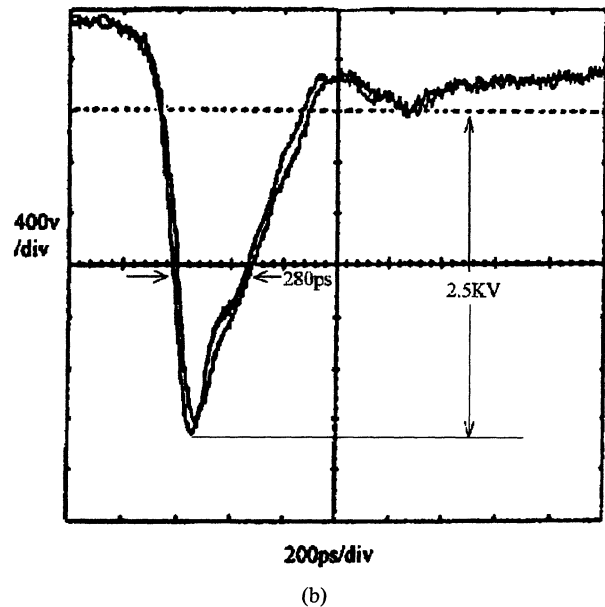
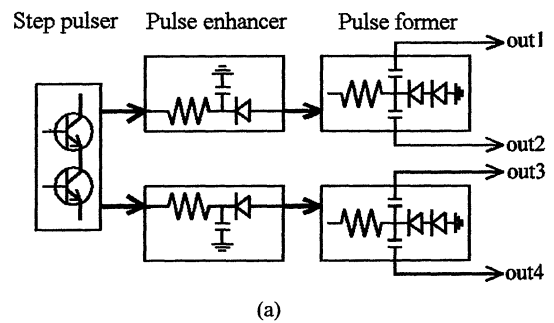


Fig. 3. Gating pulses and pulse circuit. (a) Diagram of the pulser. The first avalanche transistor outputs two step pulses in parallel. The step pulses were modified by the second stage of the pulse enhancer, and drove the pulse former to generate four gating pulses. (b) Output 1 and output 3 of the circuit. The measurement was carried out with Tek 11801A sampling oscilloscope.

was carried out with a TEK 11801A sampling oscilloscope and HV attenuators of Barth Inc. The generated four gating pulses were 280 ps FWHM and 2.5 kV amplitude in 50 Ω load. The resultant amplitude applied on the stripline cathode on the MCP was over 1 kV.

Jitters between pulses were determined by the stability of the two diode circuits of the 2nd and 3rd stages. Only the first stage of the avalanche transistor was applied with power, the passive circuit of the 2nd and 3rd stages possessed good stability and induced few jitters. Therefore, the jitters between pulses were small.

We also measured the jitters of the circuit with a TEK SCD 1000 oscilloscope during the laser plasma experiment. The measured jitters between the pulses and triggering signal were less than 50 ps, and jitters between different pulses were very small and could not be identified. Therefore, the four gating pulses showed a good synchronicity.

2.3 System structure

The layout of the whole system is shown in Fig. 1. The MCP imager is welded on a flange and covered by a shielding case. The shielding case is fixed on the flange and prevents

noise, light and electromagnetic disturbance on MCP during the laser plasma experiment. The UV and illuminating light are mounted inside the shielding case. The pinhole system is fixed outside the shielding case. The system was designed to obtain images and spectra (with pinhole grating) with $20\times$ to $2\times$ magnification for the vacuum chamber radius of 563 to 800 mm. The distance between the cathode to the target could be prolonged to 1.8 m with an additional vacuum system to obtain better spectral resolution.

For the alignment of the pinhole array to stripline cathodes, the pinhole adjustment system with both manual and stepping motor controls is mounted in front of the imager. There is also a rotating device in front of the stepping motors to adjust the orientation of the pinhole array. The precision of the stepping motor is $5\ \mu\text{m}/\text{step}$, and its limit of adjustment is $\pm 3\ \text{mm}$. An additional manual adjuster has a coarse adjustment range of $\pm 13\ \text{mm}$. The stepping motor is controlled by a control box or a personal computer connected to the control unit. Therefore, the position of the pinhole array can be adjusted out of the vacuum chamber during the experiment. The magnification of the pinhole imaging can be changed by adjusting the telescopic shaft.

During pinhole adjustment, it is difficult to observe the tiny pinholes without good illumination. We installed a movable illuminating light in the shielding case as shown in Fig. 1(b). A mark was introduced at the center of the MCP to act as the base point for the alignment. The pinholes can easily be observed when the light is moved on the axis of the target/MCP. The center mark and striplines on MCP can be illuminated when the light is moved outside the axis.

In the experiment, we first set up the alignment base axis passing the target and the center mark on the MCP with a microtelescope. With the help of the illuminating light, it is easy to observe the center mark on the MCP. After the base axis was established, we put on the pinhole array and moved the illuminating light on the axis. Thus, the pinholes could be seen clearly and adjusted to the correct position.

The control unit outputs four gating pulses of 2.5 kV amplitude and 280 ps FWHM to gate the MCP. Besides varying the voltage/MCP gap, the camera gain can also be adjusted by applying a bias on the MCP, as shown in Fig. 1. The camera is designed with 5 step MCP bias voltages. We measured the time resolution with a frequency quadrupled CPM Nd:YAG laser system.^{5,6)} The measured exposure time of the camera ranges from 60 ps to 100 ps, corresponding to different MCP bias values in the range from 90 V to $-90\ \text{V}$.

We designed three steps of the voltage applied to the MCP/screen gap of 2.6 kV, 3.5 kV and 4.5 kV. The camera can be operated with 2.6 kV at vacuum of 7.5×10^{-5} Torr without breakdown. The voltage can be set to 4.5 kV at a high vacuum of 2.5×10^{-5} Torr to obtain the best gain and spatial resolution. The UV light installed in the shielding case can be used as the light source to perform in-situ examinations when the MCP is applied with $-600\ \text{V}$ DC bias. A moveable filter shelf at the entrance of the shielding case can be applied to a multilayer of filters for each stripline [as shown in Fig. 1(b)].

The transmission time from the center of the MCP to the output connectors was precisely measured by means of an oscilloscope. It is possible to precisely observe the timing relation between output gating pulses and an XRD or PIN signal in a oscilloscope. That is very useful for synchronizing the

camera with the X-ray signal. It can also be used to resolve the time sequence of measured images with the laser or X-ray.

2.4 Application

The entire camera system is routinely used in laser plasma experiments. In the experiment, the system shows high stability and operating convenience. Figure 4 shows two of the experimental results of different target types with pinhole array and pinhole grating array respectively. In the experiment, the camera was operated at phosphor screen voltage of 4.5 kV and the exposure time of 80 ps. The magnification of the pinhole imaging was $10\times$ and the distance from target to the MCP cathode was 568 mm. The laser in the experiment is a frequency tripled Nd:YAG laser with energy of $\sim 50\ \text{J}$.

Figure 4(a) shows successive frames of evolution of plasma in a hollow target with an observation slit. The slit was made for observing the plasma evolution inside the target. The diameter of the 12 pinholes is $30\ \mu\text{m}$. The time sequence of the 12 frames is 0, 55 ps, 110 ps, 500 ps, 555 ps, 610 ps, 1 ns, 1.055 ns, 1.11 ns, 1.5 ns, 1.555 ns, and 1.61 ns.

Figure 4(b) shows the temporal, spatial and spectrally resolved results for a double disk target. The target is composed of a pair of Au disks separated by $\sim 50\ \mu\text{m}$. During experiment, the laser was targeted onto one disk. The evolution of plasmas from this disk to the other disk was recorded

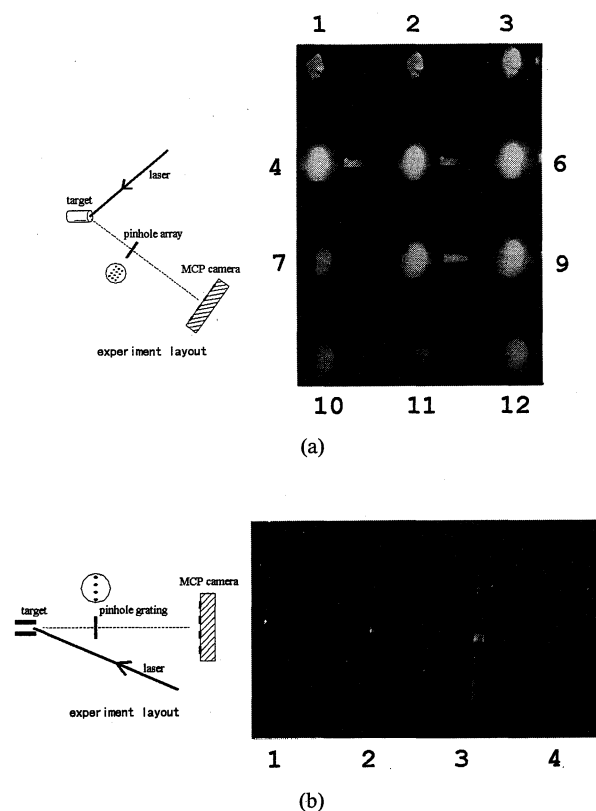


Fig. 4. Laser experiment results. The exposure time of each frame is 80 ps. The incident laser is a frequency tripled Nd:YAG with energy $\sim 50\ \text{J}$. (a) Temporally resolved observation of a slit target with a 12-pinhole array. The time sequence of the 12 frames is 0, 55 ps, 110 ps, 500 ps, 555 ps, 610 ps, 1 ns, 1.055 ns, 1.11 ns, 1.5 ns, 1.555 ns, and 1.61 ns. (b) Temporally and spectrally resolved observation of double disk target with a 4-pinhole grating array. The time sequence of the four frames is 0, 250 ps, 500 ps, and 750 ps.

such that all the time, spatial and spectral parameters were resolved. The pinhole grating was 50 μm in diameter with 1500 lp/mm grating. The time sequence of the four frames was 0, 250 ps, 500 ps, and 750 ps.

3. Summary

We have constructed a gated MCP camera system for laser plasma experiments. The camera has four 6-mm-wide stripline cathodes on the MCP, and is capable of capturing multiframe soft X-ray images. The time resolution of the system was measured to be 60–100 ps with +90 V to –90 V bias voltage applied to the MCP. The measured spatial resolution of the imager was 15 lp/mm with 10% consistent response of the four striplines and operating convenience were major concerns in the design and construction.

A single avalanche transistor circuit was used to generate the four gating pulses for each stripline. The generated 2.5 kV, 280 ps pulses had good waveform and timing consistency. The transmission properties of the four striplines were carefully adjusted to be identical. Considering the difficulty in aligning the pinhole array to target and striplines, a pinhole system with a functional control device and a flexible illuminant was installed in the system. This proved to be highly effective for achieving the alignment and adjustment of the pinhole array.

The system was used in a high-power laser plasma experiment with both the pinhole and pinhole grating array. The experiment demonstrated that the system has high stability and reliability and is very convenient to operate.

Acknowledgments

One of the authors (B. Shan) wishes to acknowledge Professor K. Hirano of Gunma University for his valuable discussions and help with the organization of this paper. This camera was made for the Chinese Academy of Engineering Physics and is part of the state key project "Femtosecond Laser and Ultrafast Phenomena". Professor Cheng Jinxiu and Zheng Zhijian are much appreciated for their discussions in the design and help with the application.

- 1) B. K. F. Yang, R. E. Stewart, J. G. Woodworth and J. Bailey: *Rev. Sci. Instrum.* **57** (1986) 2729.
- 2) J. D. Kilkenny, P. Bell, R. Hanks, G. Power, R. E. Turner and J. Wiedwald: *Rev. Sci. Instrum.* **59** (1988) 1793.
- 3) M. Katayama, M. Nakai, T. Yamanaka, Y. Izawa and S. Nakai: *Rev. Sci. Instrum.* **62** (1991) 124.
- 4) O. L. Landen, P. M. Bell, J. A. Oertel, J. J. Satariano and D. K. Bradley: *Proc. SPIE* **2002** (1994) 2.
- 5) Z. Chang, B. Shan, X. Liu, H. Yang, W. Zhu, J. Hou and X. Gong: *Proc. SPIE* **2513** (1994) 106.
- 6) Z. Chang, B. Shan, X. Liu, W. Zhu, H. Yang, J. Liu, J. Hou and M. Gong: *Proc. SPIE* **2549** (1995) 53.
- 7) B. Shan, J. Liu, Z. Chang, X. Liu, S. Gao, Y. Ren, Y. Luo, J. Jinxiu and C. Yang: *Proc. SPIE* **2869** (1997) 182.
- 8) J. A. Ortel, T. Archuleta and C. G. Peterson: *Rev. Sci. Instrum.* **68** (1997) 789.
- 9) S. Thomas and G. Power: *Proc. SPIE* **2513** (1994) 164.
- 10) I. V. Grekhov and A. F. Kardo-Sysoev: *Sov. Tech. Phys. Lett.* **5** (1979) 395.
- 11) T. E. McEwan and R. L. Hanks: *Proc. SPIE* **1346** (1990) 465.